Proceedings of the 9th U.S. National and 10th Canadian Conference on Earthquake Engineering
Compte Rendu de la 9ième Conférence Nationale Américaine et
10ième Conférence Canadienne de Génie Parasismique
July 25-29, 2010, Toronto, Ontario, Canada • Paper No

AXIAL-SHEAR-FLEXURE INTERACTION HYSTERETIC MODEL FOR RC BRIDGE COLUMNS UNDER COMBINED ACTIONS

Shi-Yu Xu[1] and Jian Zhang[2]

ABSTRACT

This paper proposes a coupled axial-shear-flexure interacting (ASFI) hysteretic model that can capture the nonlinear interactive behavior of RC bridge columns under combined action of shear, bending moment and variable axial load. The model utilizes a novel concept of normalization to parameterize the primary curves at different axial load levels. An axial load independent stress level index at any given ductility is developed to enable the transition between different reloading and unloading branches corresponding to variable axial load levels. The model is able to realistically simulate the pinching behavior, strength deterioration and stiffness softening under combined actions. It is validated against the experimental results of columns subject to varying axial loads and shows good agreement.

1. Introduction

Under earthquake shakings, the reinforced concrete (RC) bridge columns are typically subjected to combined actions of axial, shear and flexure forces that are direct consequences of structural and geometrical constraints (e.g. skewed or curved, uneven span or column heights etc.) and the multi-directional input of earthquake motions. More importantly, the axial force in columns is changing continuously due to vertical ground motion and it can directly impact the ultimate capacity, stiffness and hysteretic behavior of shear and flexure responses owing to the axial-shear-flexure interaction (ASFI), as indicated by ample laboratorial evidences (Abrams 1987; Gould and Harmon 2002; Sakai and Kawashima 2000). The axial load fluctuations and the associated ASFI of RC columns may have adverse impacts on the overall performance of bridges. Therefore, a robust analytic model capable of realistically simulating the nonlinear interactive behavior of RC columns under the combined actions is needed.

To fully understand the mechanism behind the ASFI in RC columns, it is necessary to conduct the very detailed sectional analysis which considers the material behaviors and properties (constitution laws), the relationship between different local strain components (compatibility conditions), and the transmission of forces and stresses over the cross section (equilibrium equations). The Modified Compression Field Theory (MCFT, Vecchio and Collins 1986) is one of the pioneer studies of this kind. Many contemporary studies combine the classical fiber model (Spacone et al. 1996) with MCFT to develop new approaches that are capable of capturing both the

[1] Graduate Student Researcher, Dept. of Civil & Environmental Engineering, UCLA, Los Angeles, CA 90095
[2] Assistant Professor, Dept. of Civil & Environmental Engineering, UCLA, Los Angeles, CA 90095

axial-flexure and shear-flexure behaviors (Vecchio and Collins 1988; Mostafaei and Kabeyasawa 2007). Nevertheless, this paper is focused on the concentrated plastic hinge type model that can be used in displacement-based finite element programs. Although empirical and approximate, this type of model is relatively easy to be implemented and computationally efficient for the purpose of conducting seismic assessment of bridges.

Built upon the shear-flexure interaction scheme developed by the authors (Xu and Zhang 2009), this study proposes a nonlinear ASFI model that can account for the effects of varying axial load. By introducing the concepts of normalization of primary curves (NPC), the entire primary curve family of a column can be fully defined and estimated from any reference primary curve corresponding to a known axial load level. An axial load independent stress level index (SLI) is proposed and used to mark the effective stress level of a column at any given displacement ductility. The SLI enables the identifying of equivalent loading state subject to any axial load level; hence the transition between different unloading and reloading branches pertaining to various axial load levels can be achieved. The proposed ASFI model is validated against a column test program showing excellent agreement between the predicted and measured hysteretic responses.

2. Shear-Flexure Interaction Model of Columns with Constant Axial Load

A coupled hysteretic model to account for nonlinear shear-flexure interactive behavior of RC columns under constant axial load has been developed and validated by the authors (Xu and Zhang 2009). The proposed hysteretic model consists of a flexure and a shear spring coupled at the element level, whose nonlinear behaviors are governed by their respective primary curves and a set of improved loading/unloading rules to capture the pinching, stiffness softening and strength deterioration of columns due to combined effects of axial load, shear force and bending moment. The shear-flexure interaction (SFI) is considered both at section level when theoretically generating the primary curves using the MCFT and at element level through enforcing the local and global equilibrium at any given time. The model has been implemented as a user element in a displacement-based finite element program, ABAQUS and calibrated against a large number of column specimens from static cyclic tests to dynamic shake table tests showing excellent agreement with experiment data for both flexure and shear dominated columns. The proposed model is computationally efficient and has been used reliably in conducting realistic seismic assessment of several bridges (Zhang and Xu 2009).

Fig. 1 describes the general procedure of the SFI scheme where MCFT is used to obtain the primary curves for flexural and shear springs in the coupled hysteretic SFI model. Under the constant axial load, the moment-curvature and the shear force-shear strain relationships of the section depend on the moment-to-shear (M/V) ratio (or equivalently the aspect ratio H/D) and sectional properties (geometry, reinforcement and material etc.). Using the software, RESPONSE 2000 (where MCFT has been incorporated) and following the procedure shown in Fig.1, the primary curves and the critical points corresponding to the cracking and yielding points can be defined. Built upon the pioneering shear hysteretic model by Ozcebe and Saatcioglu (1989) and the well-known flexure hysteretic model by Takeda (Takeda et al. 1970), improved loading/unloading rules are derived, which govern the hysteretic behavior based on the loading history and critical points on the primary curve.

The axial load variation is essentially inevitable due to the vertical ground motion component. It can affect the nonlinear behavior of columns under the combined loadings in several ways. The primary curve governing the monotonic lateral force-lateral displacement

behavior will be changed with different axial load levels. For two identical RC sections subject to the same shear force and bending moment but different axial loads, the distribution of normal stresses over the cross section will be different, resulting in two distinct sets of strain fields and principal planes, according to the MCFT. These changes in turn directly affect the computed curvature and shear deformation and consequently the primary curve. Therefore, the axial load variation affects not only the lateral capacity but also the stiffness of the columns. Furthermore, the crack path in concrete material essentially follows the principal planes. The rotation of principal planes owing to various levels of axial loads will also alter the crack patterns at critical sections and contribute to the final failure modes of the RC columns. Finally, the axial load level is one of the dominant parameters that control the pinching behavior of RC columns (Ozcebe and Saatcioglu 1989; Xu and Zhang 2009). Pinching behavior is more significant when the columns are subjected to tensile or low level of compressive axial loads as a result of crack widening and closing during the load reversal. Appropriate modeling of above-mentioned effects of axial load variation is extremely important for conducting the seismic response analysis of bridges.

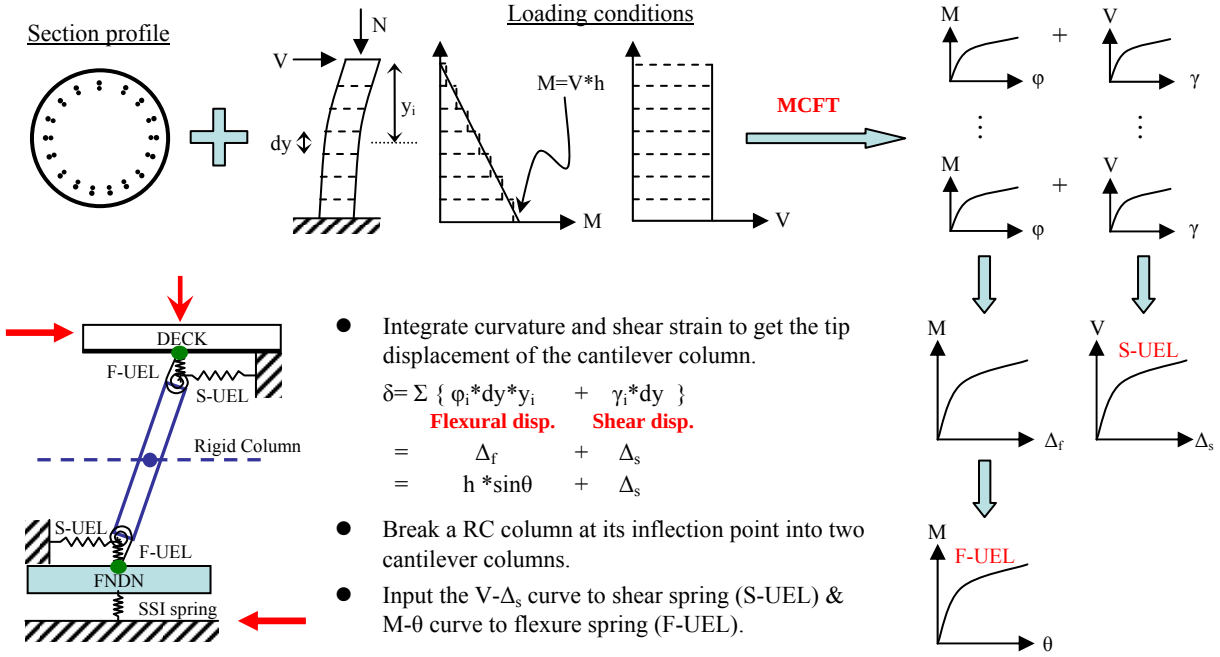

Figure 1. Implementation of the SFI scheme

3. Axial-Shear-Flexure Interaction Model of Columns with Variable Axial Load

3.1 Parameterized Primary Curves under Variable Axial Load

As discussed in the previous section, the change in primary curves due to variable axial load need to be captured in order to describe the axial-shear-flexure interaction (ASFI) behavior of columns. Fig. 2 plots the theoretically derived total primary curves of three column specimens under different axial load levels ranging from 5% tension to 20% compression of their respective nominal axial capacity. As the compressive axial load increases, the lateral resistance of the column becomes stronger and stiffer. However, the yield displacement (defined as the point on

primary curve where the stretched rebars first yield) remains almost unchanged, despite that the ultimate capacity, yielding load, and crack point all increase together with the applied axial load level, as demonstrated in Fig. 2. By normalizing the critical points (in terms of cracking displacement and force, yielding force and ultimate capacity) at given axial load levels with the yielding point of the primary curve under 5% axial compression, one can plot the normalized quantities with the applied axial load levels as shown in Fig. 3. Based on the data of three column specimens in Fig. 2, the regression equations are obtained and shown in Eqs.1 to 4. They can be used later on for generating the primary curves at any axial load level based on a reference curve, e.g. the 5% axial load curve. Therefore, the critical points and primary curves can be fully parameterized and described.

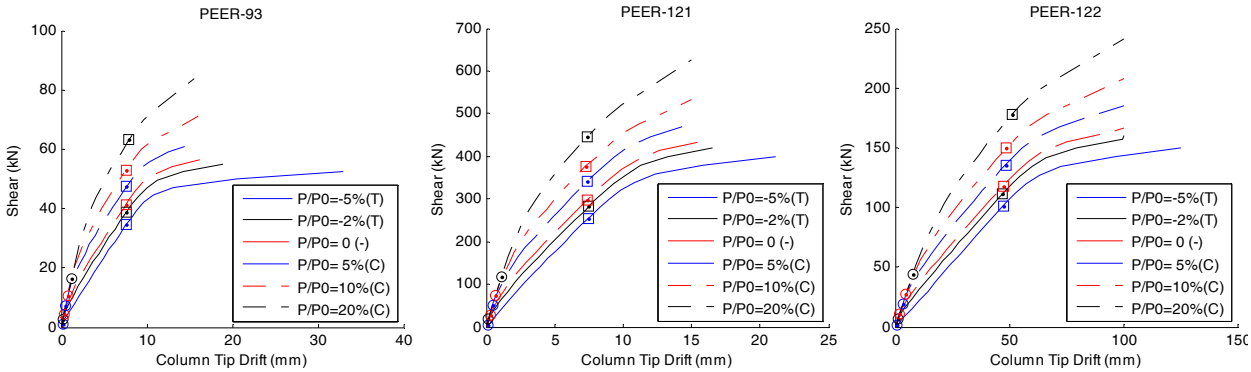

Figure 2. Critical points and total primary curves of columns under different axial loads

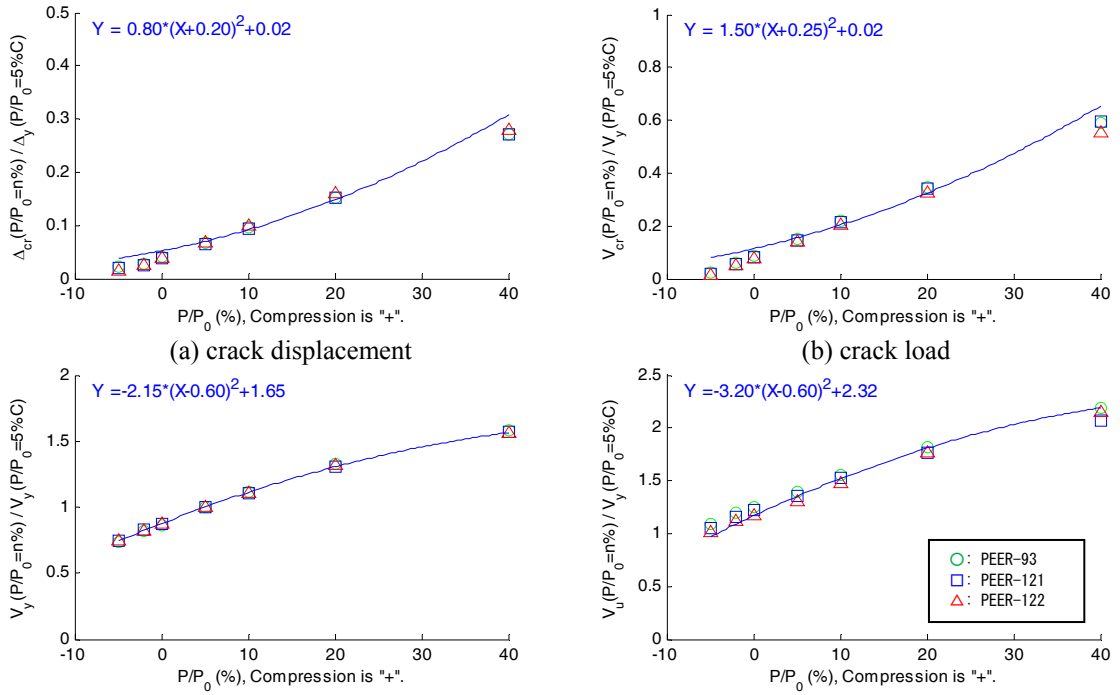

(a) crack displacement (b) crack load

(c) yield load (d) ultimate capacity

Figure 3. Variation of critical points with respect to the applied axial load

$$\frac{\Delta_{cr}(P/P_0 = n\%)}{\Delta_y(P/P_0 = 5\%)} = 0.8*(\frac{P}{P_0} + 0.20)^2 + 0.02 \quad (1)$$

$$\frac{V_{cr}(P/P_0 = n\%)}{V_y(P/P_0 = 5\%)} = 1.5*(\frac{P}{P_0} + 0.25)^2 + 0.02 \quad (2)$$

$$\frac{V_y(P/P_0 = n\%)}{V_y(P/P_0 = 5\%)} = -2.15*(\frac{P}{P_0} - 0.6)^2 + 1.65 \quad (3)$$

$$\frac{V_u(P/P_0 = n\%)}{V_y(P/P_0 = 5\%)} = -3.20*(\frac{P}{P_0} - 0.6)^2 + 2.32 \quad (4)$$

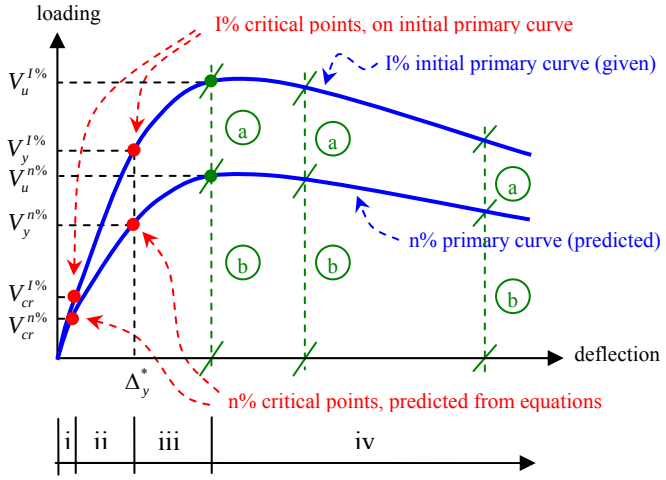

(i) 0➔crack: straight line

$$DL = def.level \equiv \frac{\Delta_{(i)}^{I\%}}{\Delta_{cr}^{I\%}} \Rightarrow \Delta_{(i)}^{n\%} = DL*\Delta_{cr}^{n\%}$$

$$SL = stress.level \equiv \frac{V_{(i)}^{I\%}}{V_{cr}^{I\%}} \Rightarrow V_{(i)}^{n\%} = SL*V_{cr}^{n\%}$$

(ii) crack➔yield: interpolation

$$DL = def.\ level \equiv \frac{\Delta_{(ii)}^{I\%} - \Delta_{cr}^{I\%}}{\Delta_y^* - \Delta_{cr}^{I\%}}$$

$$SL = stress\ level \equiv \frac{V_{(ii)}^{I\%} - V_{cr}^{I\%}}{V_y^{I\%} - V_{cr}^{I\%}}$$

$$\Delta_{(ii)}^{n\%} = DL*(\Delta_y^* - \Delta_{cr}^{n\%}) + \Delta_{cr}^{n\%}$$

$$V_{(ii)}^{n\%} = SL*(V_y^{n\%} - V_{cr}^{n\%}) + V_{cr}^{n\%}$$

(iii) yield➔ultimate: interpolation

$$ductility\ unchanged \Rightarrow \Delta_{(iii)}^{n\%} = \Delta_{(iii)}^{I\%}$$

$$SL = stress\ level \equiv \frac{V_{(iii)}^{I\%} - V_y^{I\%}}{V_u^{I\%} - V_y^{I\%}}$$

$$V_{(iii)}^{n\%} = SL*(V_u^{n\%} - V_y^{n\%}) + V_y^{n\%}$$

(iv) ultimate➔failure: constant residual strength ratio

$$ductility\ unchanged \Rightarrow \Delta_{(iv)}^{n\%} = \Delta_{(iv)}^{I\%}$$

$$RSR = residual\ strength\ ratio \equiv \frac{V_{(iv)}^{I\%}}{V_u^{I\%}}$$

$$V_{(iv)}^{n\%} = RSR*V_u^{n\%}$$

Figure 4. Rules for mapping between primary curves

Generation of the entire primary curve family under any specific level of axial load (but within the reasonable range from -5% to 40% of its own ultimate axial compressive capacity) is made possible by following the rules listed below and illustrated in Fig. 4:

(a) Yield displacement is assumed unchanged under variable axial load and the ultimate displacement is taken at ductility level of 2.

(b) Crack point, yield load, and ultimate load are estimated using Eqs.1 to 4.

(c) For a given initial primary curve associated with I% axial load, apply rules (a) and (b) to find the critical points on the 5% axial load curve. Then, use this 5% axial load curve and rules (a) and (b) again to obtain the critical points on any desired n% axial load curve.

(d) Points on the primary curves falling in between from origin to crack point [case (i) in Fig. 4], from crack point to yield point [case (ii) in Fig. 4], or from yield point to ultimate point [case (iii) in Fig. 4] are determined using linear interpolation.

(e) For points with ductility larger than the ultimate point [case (iv) in Fig. 4], the

displacement are assumed to remain unchanged but the force is varied in a way such that the load ratio between the two primary curves is kept constant and equal to the ratio at the ultimate point [i.e., b/(a+b) in Fig.4].

With the proposed normalization of primary curves and mapping rules, the idea of "shift of primary curves" (Saatcioglu et al. 1983) is no longer limited to a certain number of pre-defined primary curves associated with some prescribed levels of axial loads.

3.2 Mapping between Unloading/Reloading Branches according to Effective Axial Load

In addition to the primary curves, the unloading/reloading stiffnesses are also affected by the axial load variation. During the transient analysis of bridge response under earthquakes, the axial forces in columns will fluctuate from their initial static axial load levels and may occasionally go into the tensile side due to the vertical ground motion component (Zhang and Xu 2009). Consequently, it is also required to map between different unloading and reloading branches pertaining to various levels of axial load in a loading hysteresis. A crucial assumption is developed, which states that the effective lateral stress level of a loaded column at the fixed displacement ductility is independent of applied axial load. This assumption dictates that for a RC column subject to a prescribed lateral loading history, although the axial load variation at the current loading stage may change its lateral capacity, as long as there is no further change in lateral deflection, the ratio of effective lateral load to the lateral capacity on the primary curve will remain the same. A stress level index (SLI) is therefore defined as the current lateral load on the unloading/reloading branches divided by the lateral load on the primary curve associated with the maximum experienced lateral displacement, Δ_{max}, as shown below:

$$\text{Stress Level Index} = \frac{\text{Effective Lateral Load, } V_{eff}}{\text{Lateral Capacity at } \Delta_{max}, V_m} \tag{5}$$

Fig. 5 graphically explains how this axial load independent SLI works. In Fig. 5, the primary curves of the same column under three different levels of axial loads are plotted in solid blue lines. The SLI as currently shown in the figure are equal to c/d for all three cases. If the lateral deflection is fixed at Δ_1 and the axial load fluctuates among the three axial load levels, the effective lateral load will move up and down to keep the SLI as a constant (i.e., c/d in Fig.5).

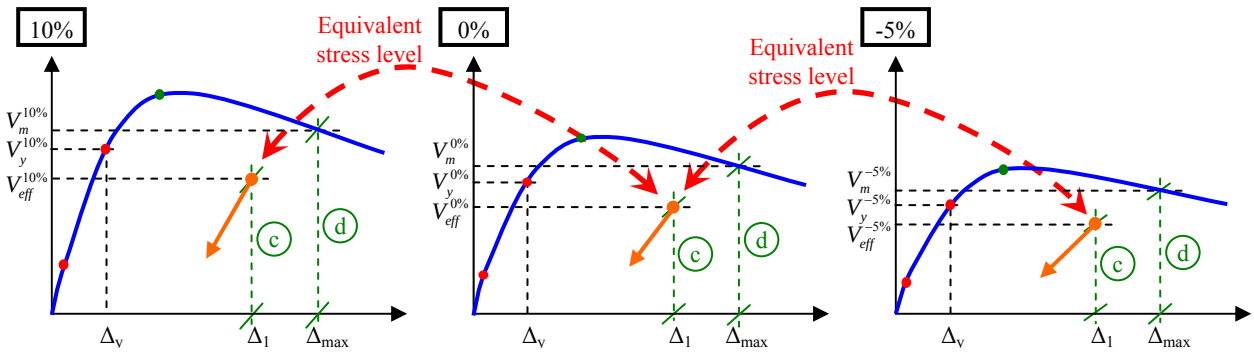

Figure 5. Rules for mapping between unloading and reloading branches

If during the analysis, both the axial load and lateral deflection have been varied from the previous time increment, the loading state at current time increment can be broken into two sub-stages: the constant lateral deflection stage and the constant axial load stage. This two-stage loading approach is illustrated in Fig. 6. In the first sub-stage (constant lateral deflection), the lateral deflection is forced to keep constant thus the effective lateral load will move only upward or downward to stay at the same SLI [in this example, equal to c/d]. Next in the second sub-stage (constant axial load), it is the axial load that is forced to keep constant so the hysteretic SFI models (aforementioned in section 2) can be applied to determine the loading state on current unloading or reloading branches. The two-stage loading approach requires no local iteration to solve for the lateral loads and lateral stiffnesses, therefore it is a much more efficient solution approach than the fiber section approaches.

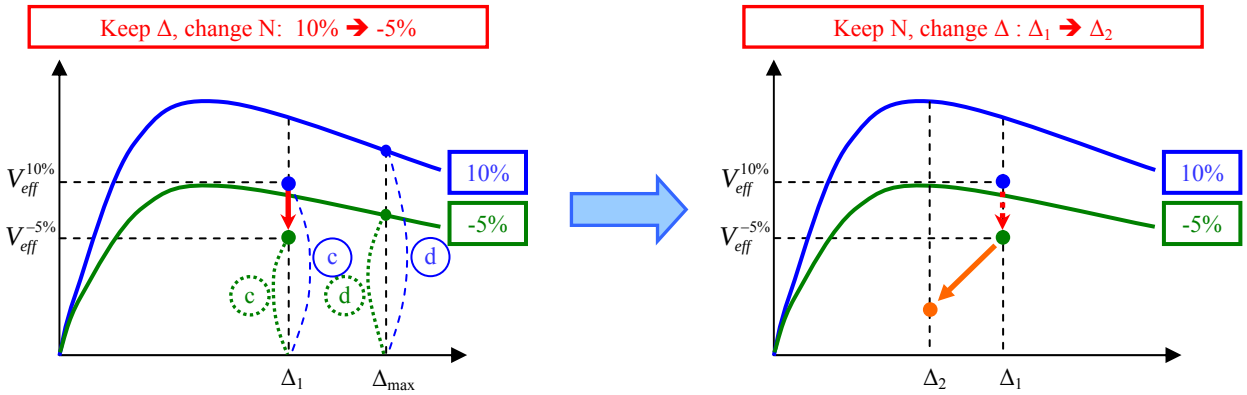

Figure 6. Illustration of constant lateral deflection (left) and constant axial load (right) stages

4. Model Validation

Four RC columns (Sakai and Kawashima, 2000) with identical dimensions (400mm x 400mm square section, 1350mm in height, with effective depth =360mm), reinforcement (longitudinal reinforcement ratio =1.58%, transverse reinforcement ratio = 0.79%), and material strength (f_c'≈23.0MPa, $f_{y,longi.}$=374MPa, $f_{y,tie}$=363MPa) tested under controlled displacement hysteresis and under various axial load conditions were used to validate the proposed axial-shear-flexure interaction modal. The configuration of applied axial loads in the test program is listed in Table 1. The axial load in specimen TP-031 was kept constant in compression at 12.8% of its ultimate axial capacity while that in specimen TP-032 was kept constant at -4.62% (tension). The axial loads in the last two specimens, TP-033 and TP-034, vary in phase with the applied lateral displacement. Loading hystereses of specimens TP-033 and TP-034 are plotted in Fig. 7.

Table 1. Applied axial loads in the experimental test program

	TP-031	**TP-032**	**TP-033**	**TP-034**
Axial Force (kN)	+470 (constant)	-170 (constant)	-10 ~ 310	-170 ~ +420
Axial Load Ratio	+12.8% (Comp.)	-4.62% (Tension)	-0.27%T ~ +8.5%C	-4.62%T ~ +11.4%C

To validate the proposed rules for mapping of primary curves among distinct axial loads, the envelope of the hysteretic response of specimen TP-031 (axial load level = +12.8%C) is

input as the initial primary curve to the model, then the prediction on the hysteretic response of TP-032 (axial load level = -4.62%T) is made and compared with the experimental data. Similar evaluation is made on the hysteretic response of TP-031 when the envelope of TP-032 is input into the system as the initial primary curve. The predicted hysteretic responses (dot red lines) of the two cases are plotted in Fig. 8, together with the experimental data (solid blue lines). The good agreement between the predicted and experimental loops indicates that the proposed mapping rules are appropriate to parameterize the entire primary curve family for RC columns.

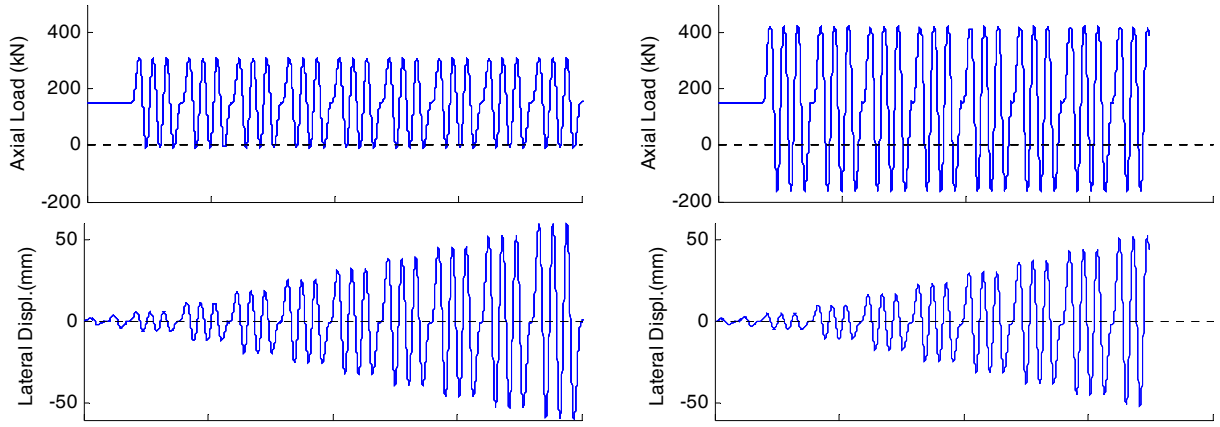

(a) TP-033 (b) TP-034

Figure 7. Axial and lateral loading hystereses applied to specimens TP-033 and TP-034

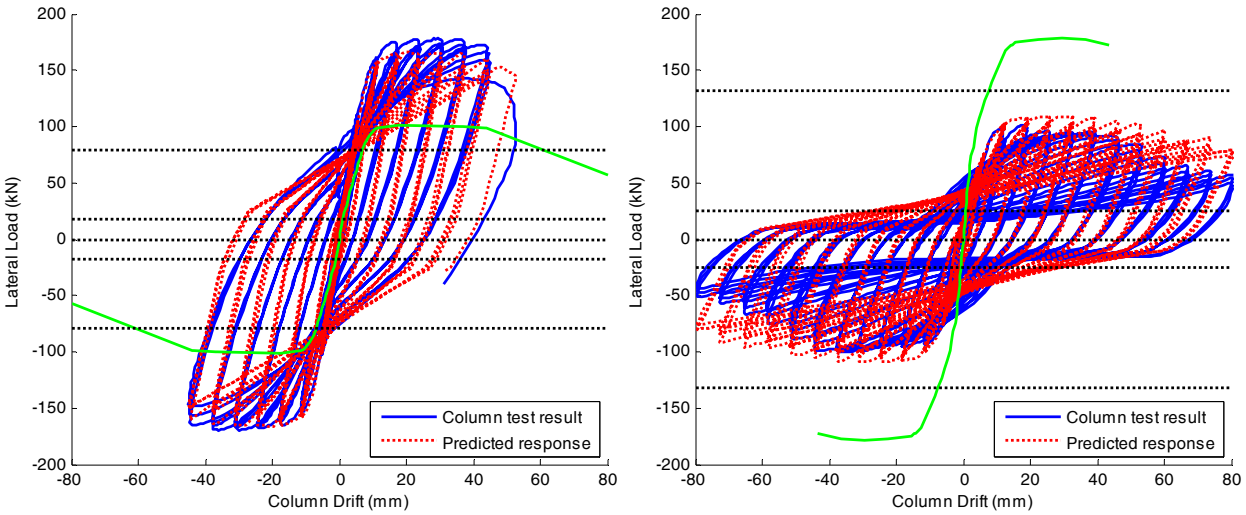

(a) Given the primary curve of TP-032, predicts the response of TP-031.

(b) Given the primary curve of TP-031, predicts the response of TP-032.

Figure 8. Hysteretic responses of specimens TP-031 and TP-032

Fig. 9(a) compares the predicted (dot red lines) hysteretic response of specimen TP-033 (axial load level varying from -0.27%T to +8.5%C) with its test results (solid blue lines), when the envelope (bold solid green line) of the hysteretic loops of specimen TP-031 (axial load level

= 12.8%C constant) is input as the initial primary curve. Similar comparison of the specimen TP-034 (axial load level varying from -4.62%T to +11.4%C) is shown in Fig. 9(b), in which the envelope of TP-032 (axial load level = -4.62%T constant) is used as the initial primary curve. The good agreement between the predicted and experimental loops in both cases validates the idea of axial load independent stress level index and the proposed two-stage loading approach.

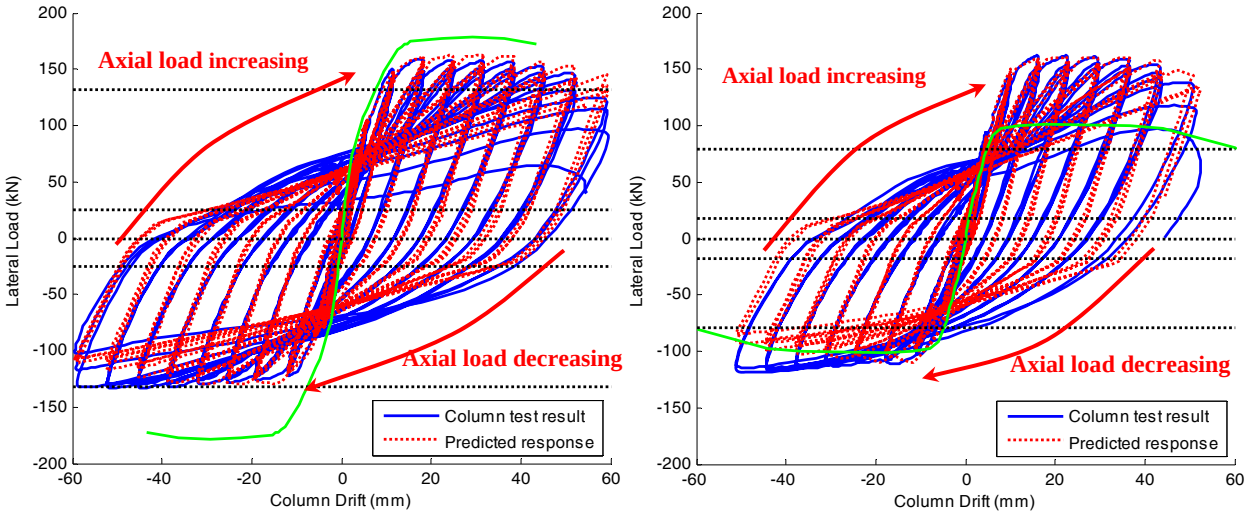

(a) Given the primary curve of TP-031, predicts the response of TP-033.

(b) Given the primary curve of TP-032, predicts the response of TP-034.

Figure 9. Hysteretic responses of specimens TP-033 and TP-034

It is noteworthy that the lateral capacities of specimens TP-033 and TP-034 are different in the two opposite loading directions. In these two tests, the axial load is increasing as the column is deformed to the right, and it keeps decreasing when the column is pulled back to the left. The capacity is larger when the applied axial load level is higher, and vice versa. It is clear that the axial load variation does have a crucial effect on the lateral response of RC columns.

5. Conclusions

Axial load variation in a RC column can alter its stiffness, ultimate capacity, and hysteretic responses. A shear-flexure interaction scheme previously developed by the authors for modeling the responses of RC columns subject to constant axial load is enhanced in this study to enable the consideration of varying axial load. By applying the novel concept of normalization of primary curves, the entire primary curve family of a RC column under various levels of axial load can be retrieved from any reference primary curve subject to a known axial load. Transition among unloading and reloading branches pertaining to different axial load levels during loading reversals is made possible by adopting the proposed two-stage loading approach. The two-stage loading approach includes a constant axial load and a constant lateral deflection sub-stages. It requires no local iteration to determine the tangent stiffness and lateral load and therefore suitable for spatially complicated multi-degree-of-freedom systems. The proposed ASFI model has been validated against a column test program showing very good comparisons between the predicted and observed hysteretic responses. The ASFI model can be used to simulate the

realistic behavior of bridge columns, and it provides an alternative approach other than the more complicated fiber models to efficiently conduct the transient analyses of bridge systems subject to both the horizontal and vertical components of ground motion.

Acknowledgments

The research presented here was funded by National Science Foundation through the Network for Earthquake Engineering Simulation Research Program, grant CMMI-0530737, Joy Pauschke, program manager. Any opinions, findings and conclusions or recommendations expressed in this paper are those of the authors and do not necessarily reflect the views of the National Science Foundation (NSF).

References

Abrams, D.P., 1987. Influence of axial force variations of flexural behavior of reinforced concrete columns, *ACI Structural Journal* 84(3), 246-254.

Gould, N.C., and T.G. Harmon, 2002. Confined concrete columns subjected to axial load, cyclic shear, and cyclic flexure – part II: experimental program, *ACI Structural Journal* 99(1), 42-50.

Mostafaei, H., and T. Kabeyasawa, 2007. Axial-shear-flexure interaction approach for reinforced concrete columns, *ACI Structural Journal* 104(2), 218-226.

Ozcebe, G., and M. Saatcioglu, 1989. Hysteretic shear model for reinforced concrete members, *Journal of Structural Engineering* 115(1), 132-148.

Saatcioglu, M., A. Derecho, and W.G. Corley, 1983. Modeling hysteretic behavior of coupled walls for dynamic analysis, *Earthquake Engineering & Structural Dynamics* 11, 711-726.

Sakai, J., and K. Kawashima, 2000. Effect of varying axial loads including a constant tension on seismic performance of reinforced concrete bridge columns, *Report No. TIT/EERG 00-2*, Tokyo Institute of Technology, Tokyo, Japan.

Spacone, E., F.C. Filippou, and F.F. Taucer, 1996. Fibre beam-column model for non-linear analysis of R/C frames: part I. formulation, *Earthquake Engineering & Structural Dynamics* 25(7), 711-725.

Takeda, T., M.A. Sozen, and N.N. Nielsen, 1970. Reinforced concrete response to simulated earthquakes. *Journal of Structural Division*, ASCE 96(12), 2557-2573.

Vecchio, F.J., and M.P. Collins, 1986. Modified compression-field theory for reinforced concrete elements subjected to shear, *Journal of the American Concrete Institute* 83(2), 219-231.

Vecchio, F.J., and M.P. Collins, 1988. Predicting the response of reinforced concrete beams subjected to shear using modified compression field theory, *ACI Structural Journal* 85(3), 258-268.

Xu, S.-Y., and J. Zhang, 2009. Hysteretic shear-flexure interaction model of reinforced concrete columns for seismic response assessment of bridges, *Earthquake Engineering & Structural Dynamics*, tentatively accepted.

Zhang, J., and S.-Y. Xu, 2009. Seismic response simulations of bridges considering shear-flexural interaction of columns, *Structural Engineering and Mechanics* 31(5), 545-566.